JJMIE

Volume 19, Number 1, March. 2025
ISSN 1995-6665
Pages 215– 228
https://doi.org/10.59038/jjmie/190117
Editor-in-Chief: Prof. Ali M. Jawarneh

Jordan Journal of Mechanical and Industrial Engineering

Analyzing the Effects of Axially Defective Blades on Wind Turbine Performance Optimization Using Taguchi-based Grey Relational Analysis

Abdulhamid Hamdan Al-Hinai*[1], Karu Clement Varaprasad[1], V. Vinod Kumar[1]

[1]Department of Mechanical and Mechatronic Engineering, Sohar University, Sohar, Sultanate of Oman

Received 26 Oct 2024 Accepted 8 Dec 2024

Abstract

Wind energy is essential in advancing sustainable power generation. However, the presence of vibrations in modern wind turbines poses significant challenges, leading to reduced component lifespan and operational failures. This study investigates the effects of axial surface cracks on turbine blades and variations in shaft rotational speeds on the performance of a lab-scale wind turbine simulator. The primary objective of this study is to optimize parameters for minimizing vibration and maximizing power output. A full factorial Taguchi design integrated with grey relational analysis was employed for the experimental setup. Regression models were developed using Minitab software to quantify the relationship between crack sizes, rotational speeds, and their impact on vibration levels and power generation. The optimal input setting is at a crack size of 48 mm and a rotating speed of 150 rpm, leading to a power output of 25.575 W at a vibration range of 10.896 m/s^2. The coefficients of determination (R-squared) values are found to be above 99% for best-fit model. This result indicates that larger axial crack sizes lead to a considerable decrease in power output at equivalent shaft rotational speeds. This highlights the importance of effective speed management and vibration mitigation strategies. The findings emphasize the need for robust condition monitoring systems to enhance turbine reliability and efficiency. Future research should explore advanced optimization algorithms and incorporate additional variables such as ambient conditions and real-time monitoring data, to contribute to the development of more efficient and resilient wind energy systems.

Keywords: Axial defect, Crack size, Power Output, Rotational Speed, Vibration analysis, Wind turbine blade.

Abbreviations:

SQ: Spectra Quest
WTS: Wind turbine simulator
VQ: Vibra Quest

1. Introduction

Wind energy has rapidly become an important component of the global renewable energy landscape, with a strong emphasis on enhancing efficiency and reliability to support its extensive adoption [1]-[3]. The industrial evolution from constant-speed wind turbine systems to variable-speed generators, and more recently, to brushless generators with full converters, underscores the ongoing pursuit of innovation [4][5]. Direct-drive systems, particularly valued for their reliability, are now favoured in wind turbine applications. As wind power integration into the electrical grid increases, advanced power technologies are being developed to address the associated challenges and improve turbine performance [6]. The growing significance of wind energy has further heightened the focus on reliability and availability.

Wind turbines are complex machines engineered to convert wind energy into electrical power [7]. These turbines typically comprise several key components, including the blade, rotor, shaft, generator, and gearbox. Horizontal-axis wind turbine types, which dominate the marketplace, commonly have three blades and excessive-speed asynchronous generators [5][8]. The running precept involves wind exerting dynamic strain on the blades inflicting the rotor to rotate[9]. This mechanical strength is finally converted into electrical energy with the aid of the generator. The efficiency of this conversion process depends on several critical parameters. The blades are responsible for transforming wind energy from kinetic to mechanical form. They are important for the durability and performance of wind turbine systems. They bear considerable mechanical hundreds and environmental pressures in the course of their operational durations [10]. Despite considerable improvements in wind turbine generation, the blade's defects due to one of the kinds of cracks remain a persistent trouble [11]. They have an effect on the performance and sturdiness of wind turbine structures [12]. These defects result in extended protection prices, operational downtime, and even capability protection dangers [13] [14].

* Corresponding author e-mail: abdulhamidalhinai@gmail.com.

Given the critical nature of fatigue in wind turbines, the components like blades and blade joints are particularly susceptible to failure. Fatigue analysis has then become a critical issue of the design process. It is aimed at predicting service life and enhancing reliability [15]. Crack formation in blades typically occurs mainly in three steps: crack initiation, stable crack extension, and eventual fracture[9][11]. The total fatigue life of a blade can be computed as the total crack initiation life and crack propagation life.

$$N_{total} = N_{initiation} + N_{propogation} \quad (1)$$

Wind turbine vibrations present a huge challenge[16]. They are affecting both overall performance and longevity. Aerodynamic forces, mechanical imbalances, and structural defects are the commonplace sources of those vibrations[9]. They can bring about decreased element lifespans and potential failures [17][18]. Various control strategies have been developed to mitigate these problems. Vibration monitoring plays an essential position in fault detection and analysis [19][20]. Sensors which include accelerometers are often used to measure vibrations[16]. The statistics collected are analyzed, such as the usage of special strategies like Fourier Transform, envelope evaluation, and regression evaluation [17][21]. Advanced software tools and artificial intelligence are increasingly more employed for characteristic extraction and fault recognition. They enable early warning for maintenance and prevent unexpected breakdowns [22].

Studies for monitoring blade conditions continued to push the envelope in wind turbine studies[23]. Dhanraj et al. (2017) proposed an advanced method the use of the transmissibility of frequency response capabilities to come across blade damage by using alerts acquired from multiple sensors [24]. Ou et al. (2017) addressed the crucial problem of icing on blades through introducing an shrewd detection approaches the usage of SCADA statistics [25]. Liu et al. (2019) similarly contributed by exploring non-contact thermography strategies for detecting blade icing, presenting valuable insights into subsurface fault detection [26]. Shaymaa et al. evaluated the impact of surface treatment on the turbine blade performance [23]. Additionally, Yang et al. (2015) underscored the significance of structural health monitoring in comparing wind turbine blades, at the same time as Antoniadou et al. (2015) highlighted the complexities of fault detection in wind turbine settings [27][28]. Meanwhile, Florian et al. (2015) proposed a blade time assessment model intended at improving preventive upkeep planning [29].

Experimental setups, including wind turbine simulators, are widely used in research to study wind turbine vibrations and performance under a set of controlled conditions [30]. These studies have examined the impact of movement uniformity on vibration and power generation [31]. Aeroelastic simulations have highlighted the need of precise modelling in identifying potential issues related to frequent vibrations [32]. Novel approaches have been developed to reduce vibration and noise levels, in order to address real-world vibration problems [16][33].

Regression modelling and optimization techniques are extensively used and applied in wind energy research[34]. Regression models predict wind turbine performance metrics and model power curves[21], along with advanced techniques like Extreme Gradient Boosting. They show a promise in forecasting power output based on wind velocity [35]. Optimization methods, including different computing techniques[34], are used to optimize wind farm layouts for enhanced efficiency [36]. Sensitivity analysis, critical in environmental modelling, is applied in wind turbine studies to assess the impact of input variations on outputs, contributing to the robustness and accuracy of performance models [37][38].

This study introduces a novel approach to optimizing field power output and minimizing vibration levels in wind turbine systems by conducting a Taguchi-based Grey Relational analysis of a wind turbine simulation system, which is equipped with axially defective blades operating at various rotational speeds [5][39]. Unlike previous studies, this research incorporates a condition monitoring approach to address the interplay between blade defects and operational dynamics. The primary goal is to identify the optimal operational settings that maximize power output [40] while significantly reducing vibration levels [16]. As wind turbines continue to increase in capacity and complexity, this work highlights the critical importance of proactive maintenance strategies, enabled by condition monitoring. This ensures sustainable and efficient energy production [41]. The novelty lies in the experimental integration of defect-driven vibration analysis with optimization techniques, in order to provide a practical framework for enhancing turbine performance in real-world scenarios.

This research paper is structured as follows: Section 2 presents the methodology used in the study, including the simulation setup and data analysis techniques. Section 3 discusses the results and findings, with a focus on the optimization of power output and vibration reduction[34]. Finally, Section 4 concludes the study, highlighting its contributions to the field and suggesting directions for future research.

2. Methods and Materials

Real wind speed data from Sohar town, Oman, was used as a hypothetical operating range of shaft rotational speed utilizing WTS conversion in order to examine the performance of a wind turbine simulator (WTS). The Vibra Quest (VQ) simulation software and data collection system were utilized in the Spectra Quest (SQ) type WTS model utilized in this study. The goal of this investigation was to lower the vibration waveform range's generated average. As seen in Figure 1, this is fundamentally the difference between the average of (m) positive peaks and the average of (n) negative peaks. The WTS performance improved when the vibration range was decreased. The average of positive peaks, the average of negative peaks and the vibration rangewere determined using the following equations:

$$\text{Avgerage of positive peaks} = \frac{\sum_{i=1}^{m}(\text{positve vibration peaks})}{m} \quad (2)$$

$$\text{Avgerage of negative peaks} = \frac{\sum_{i=1}^{n}(\text{negative vibration peaks})}{n} \quad (3)$$

$$\text{Vibration Range} = \text{Avgerage of positive peaks} - \text{Avgerage of negative peaks} \quad (4)$$

This section consists of: 1) an experimental layout of the SQWTS, 2) the Taguchi design of experiment (DoE), 3)Experimental works on the WTS as per DoE, 4) analyzing the generated results of vibration waveform and power output, 5) analyzing Taguchi responses, 6) regression modelling of vibration level and power output, and finally 7) optimizing the multi-responses using Grey

Relational Analysis. Figure 2 shows the methodology flow chart.

Experimental setup: As seen in Figure 3, the SQ WTS used in this study was a horizontal axis wind turbine with three blades. Its weight was 222.7 kg, its centreline height was 2.369 m, its sweeping blade diameter was 3.3 m, and its base measurements were 2.991 m × 2.438 m. As seen in Figure 4, a tachometer and an accelerometer were installed on the rotational shaft to detect the vibration level and rotational speed in one direction of vibrational stimulation [35][16], respectively. As shown in Figures 3 and 4, the SQ WTS was equipped with an accelerometer and a tachometer to measure vibration levels and shaft rotational speeds, respectively. The accelerometer used was a piezoelectric type with a sensitivity of 100 mV/g. The frequency response rangesfrom 1 Hz to 10 kHz, and the measurement accuracy was ±1% of the full scale. This high sensitivity and broad frequency response ensure accurate detection of vibration signals, including both low-frequency and high-frequency components. Whereas, the tachometer used for measuring shaft rotational speed had a resolution of 0.1 RPM and an accuracy of ±0.05% of the measured value. This level of precision is considered in this research study for capturing variations in shaft speed under different experimental conditions. The signals from these sensors were read by a data collecting system, which then transmitted them to the VQ simulation program for analysis and vibration report generation, as shown in Figure 5. Figure 6 displays the three axially cracked blades that were utilized in this study.

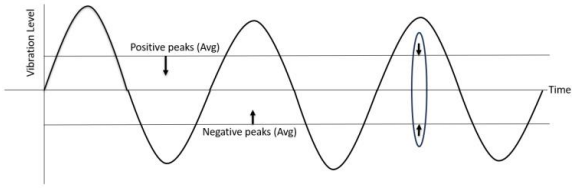

Figure 1. Research work concept

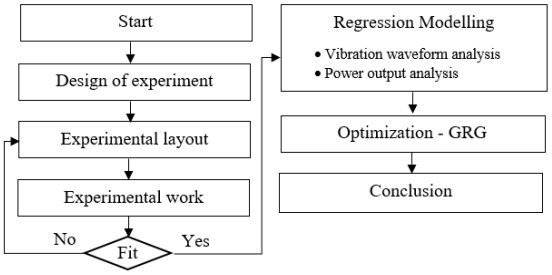

Figure 2. Methodology flow chart

Figure 3. SQ WTS

Figure 4. An accelerometer mounted on SQ WTS

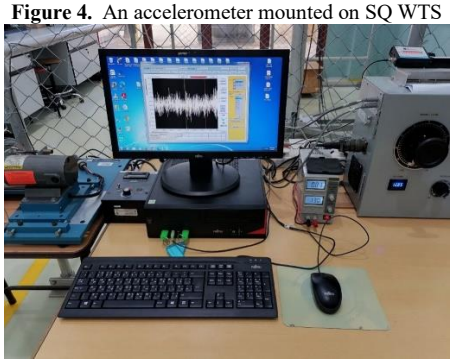

Figure 5. VQ analysis software

Figure 6. Three axial defective blades

Taguchi Design of Experiment: The two primary independent parameters were used to plan the experimental work, the shaft rotational speed (x_2) and the crack size (x_1) in a Taguchi design of experiment (DoE)[42]. The independent input parameters and their levels are displayed in Table 1. As a hypothetical operational range of Sohar wind speed utilizing WTS conversion ratio, the axial crack size ranged from 48 mm to 90 mm and eventually to 340 mm, while the shaft rotational speed varied from 50 rpm to 100 rpm and finally to 150 rpm. The selection of crack sizes (48 mm, 90 mm, and 340 mm) as levels for the factor *x*1 in the Taguchi design of experiments was based on the realistic representation of blade damage rationale. These values were chosen to represent varying degrees of transverse defects commonly observed in wind turbine blades during operation. The range covers small (48 mm), moderate (90 mm), and severe (340 mm) damage scenarios. This provided a comprehensive analysis of how crack size impacts vibration and power output.An experimental layout based on L9 orthogonal array (nine experimental experiments according to the DoE) were conducted in total. The experimental setup based on the L9 orthogonal array is displayed in Table 2. The generated vibration range (average of positive and negative peaks) and power output were the answers.

Table 1. Input parameters and their levels

Factors	Independent Parameters	Level 1	Level 2	Level 3
x_1	Crack size (mm)	48	90	340
x_2	Shaft rotational speed (rpm)	50	100	150

Table 2. Experimental layout based on L9 orthogonal array

Experiments	Crack size, x_1 (mm)	Shaft rotational speed, x_2 (rpm)
1	48	50
2	48	100
3	48	150
4	90	50
5	90	100
6	90	150
7	340	50
8	340	100
9	340	150

*Experimental testing of the WTS as per DoE:*This required replacing one of the three blades in a methodical manner with one that had an axial fault[39][43]. As seen in Figure 6, the damaged blades had cracks of 48 mm, 90 mm, and 340 mm, respectively. The 48 mm cracked blade was tested initially at 50 rpm, then 100 rpm, and lastly 150 rpm for the shaft rotation speed. For the 90 mm and 340 mm cracked blades, respectively, the same testing was conducted again.

Vibration waveform and power output analysis: The data acquisition system received the vibration signals from the accelerometer and forwarded them to the VQ software, which produced the vibration report in MS Excel format. For every test, a specific set of vibration waves (positive and negative waveform peaks) was displayed in the created report. These waves are then used for vibration analysis. The three-phase field-controlled alternator of the WTS generated the power output, which consisted of voltage and current. The voltage and current displayed on the WTS control interface represented the power output.

Regression modelling: The following regression models were created by doing regression modelling for power output and vibration ranges: linear, linear and squared, linear and interaction, and full model[21]. The best fit regression model was determined by comparing the models' R-squared values for every response[44].

Optimization of multi-responses using Grey Relational Analysis: The goal of this research project was to reduce vibration and maximize wind turbine system performance[34]. Higher the better was the criterion for power production and the average of negative vibration peaks. In contrast, the lower-the-better criterion was applied to positive vibration peaks. The following formulae were used to normalize each response's initial sequence:

For higher-the-better criterion:

$$Y_{ij} = \frac{X_{ij} - min(X_{ij})}{max(X_{ij}) - min(X_{ij})} \quad (5)$$

For lower-the-better criterion:

$$Y_{ij} = \frac{max(X_{ij}) - X_{ij}}{max(X_{ij}) - min(X_{ij})} \quad (6)$$

where x_{ij} is the measured response, $min(x_{ij})$ is the minimum of $x_{ij}$and $max(x_{ij})$ is the maximum of x_{ij}, i is the response variables and j is the experiment number. The Deviation Sequence (distinguishing coefficient) $\Delta_{ij}$was calculated as follows:

$$\Delta_{ij} = max(Y_{ij}) - Y_{ij} \quad (7)$$

where $max(Y_{ij})$ is the expected sequence, $Y_{ij}$is the comparability sequence and Δ_{ij} is the deviation sequence of $max(Y_{ij})$ and Y_{ij}. The grey relational coefficient $\xi_{ij}$was calculated as follows:

$$\xi_{ij} = \frac{min(\Delta_{ij}) + \zeta \times max(\Delta_{ij})}{\Delta_{ij} + \zeta \times max(\Delta_{ij})} \quad (8)$$

where ζ is the differentiating coefficient, $0 \leq \zeta \leq 1$, and 0.5 is the widely accepted value. The grey relational grade GRG(γ_j) for each experiment was computed as follows, for n number of responses:

$$\gamma_j = \frac{\sum_{i=1}^{n} \xi_{ij}}{n} \quad (9)$$

If larger γ_j is obtained, then the equivalent set of process parameters is nearer to the most favourable optimal setting.

3. Results and Discussion

This section includes regression analysis and optimization of the vibration reports that the VQ software produced.

3.1. Initial observations

During the initial setup phase, early observations were conducted to assess the initial/baseline performance of the wind turbine system (WTS) with both healthy and defective blades. The detection of an axial defect in one blade was associated with heightened vibration levels and variability in power output[39]. These findings were essential for this research since they illustrated the effects of blade defects under different conditions:

- The simulator with three healthy blades demonstrated almost stable operational behaviour, characterized by low vibration levels[16]. Power output consistently rose within the expected ranges corresponding to the respective rotational speeds. The recorded vibration waveforms were almost smooth, exhibiting almost no irregularities. This indicated that the blades were balanced and functioning correctly.
- Substituting one healthy blade with an axially defective blade led to noticeable changes[23][43]. Increased vibration levels were immediately detected, which significantly affected the turbine's dynamic behaviour[9]. The vibration waveforms showed irregularities and exhibited higher peaks compared to the healthy blade configuration. Additionally, the power output with the defective blade fluctuated more, reflecting the repercussions of increased vibrations and possible energy losses[23].

3.2. Waveformanalysis results

The VQ program was used to record and analyze the vibration signals. For every test case, this software produced an intricate time-domain waveform. The vibration waveforms produced by the VQ program are shown in Figure 7. As the rotational speed rose, the vibration levels also increased.

Taking into account the Taguchi design of experiment, a thorough execution of the experimental work was carried out for 9 tests [42]. The VQ software produced a waveform report for each test that included a series of vibration waves with positive and negative peaks. Concurrently, the three-phase field-controlled alternator generated the power output (voltage and current) that was shown on the WTS control interface. The measured responses from the experimental study are displayed in Table 3. Figure 8 shows the changes in vibration range and power output.

3.3. Taguchi Response Analysis

Taguchi's response analysis is aimed at minimizing variability and designing experiments to maximize performance metrics [42][44]. Response for means and response for signal-to-noise ratios were used to examine the experimental tests on the WTS with an axially cracked blade [9]. The impact of the input process parameters on the average of positive and negative peaks, vibration range, and power output, is described in depth.

3.3.1. Taguchi's Response Analysis for the average of negative peaks

The average of the negative side of the vibration waveform peaks was examined in order to determine the impact of two process parameters: crack size (x_1) and rotating speed (x_2). The performance of the system was impacted by changes in each factor (x_1 or x_2), as demonstrated by the Mean and Signal to Noise Ratios values in Table 4. Based on the higher-the-better criterion, the study revealed that the optimal set of process parameters was (x_1-1 x_2-1). This corresponded to a crack size of 48 mm and a rotational speed of 50 rpm. Figure 9 displays the response graphs for the mean of negative peaks for Means and Signal to Noise Ratios.

3.3.2. Influence of process parameters on the average of negative peaks

Variations in the size of the cracks had a smaller effect on the values of the vibration waveform's average of negative peaks. The average values from level 1 to level 3 slightly rose. This suggested that negative peak amplitudes were slightly increased by larger cracks. On the other hand, there is a much variance in negative peaks when the rotational speed increases. Mean negative peak values highly dropped as the rotating speed increased from level 1 to level 3. The further emphasis on the importance of rotating speed over crack size in this response was provided by the Delta value of 4.596.

Table 3. Measured responses from experimental tests

	Input Parameters		Responses			
Tests	Crack Size, x_1 (mm)	Rotational Speed x_2 (rpm)	Avg. (negative peaks) (m/s^2)	Avg. (positive peaks) (m/s^2)	Vibration Range (m/s^2)	Power output (W)
1	48	50	-1.407	1.448	2.855	1.804
2	48	100	-4.962	4.718	9.680	9.794
3	48	150	-5.472	5.425	10.896	25.575
4	90	50	-1.411	1.469	2.881	1.539
5	90	100	-4.959	4.732	9.691	9.425
6	90	150	-6.014	5.911	11.924	22.950
7	340	50	-1.350	1.534	2.884	1.478
8	340	100	-5.161	4.672	9.833	8.908
9	340	150	-6.469	6.470	12.940	21.988

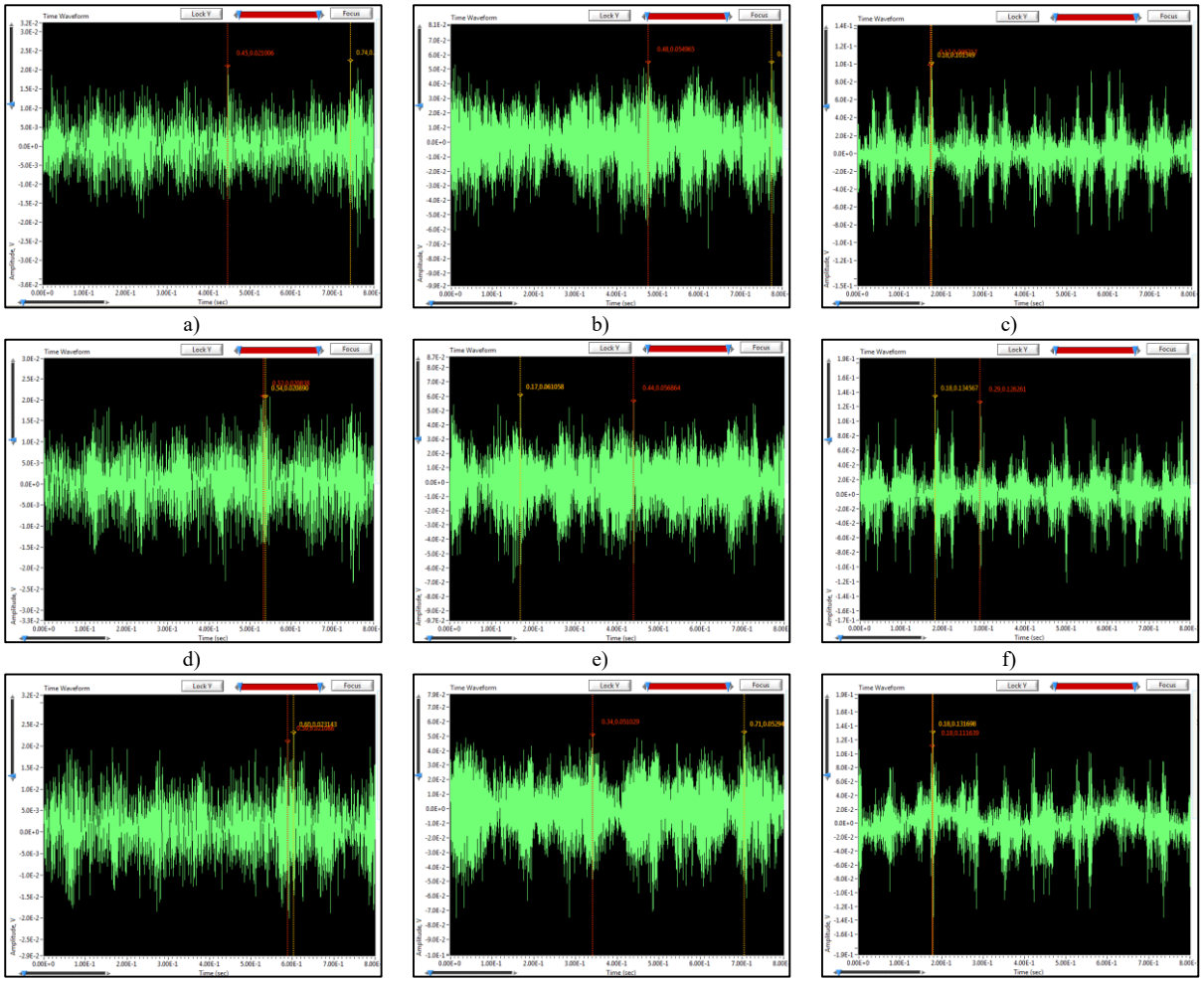

Figure 7. Vibration waveforms: a) at 50 rpm (crack size = 48 mm), b) at 100 rpm (crack size = 48 mm), c) at 150 rpm (crack size = 48 mm), d) at 50 rpm (crack size = 90 mm), e) at 100 rpm (crack size = 90 mm), f) at 150 rpm (crack size = 90 mm), g) at 50 rpm (crack size = 340 mm), h) at 100 rpm (crack size = 340 mm), and i) at 150 rpm (crack size = 340 mm)

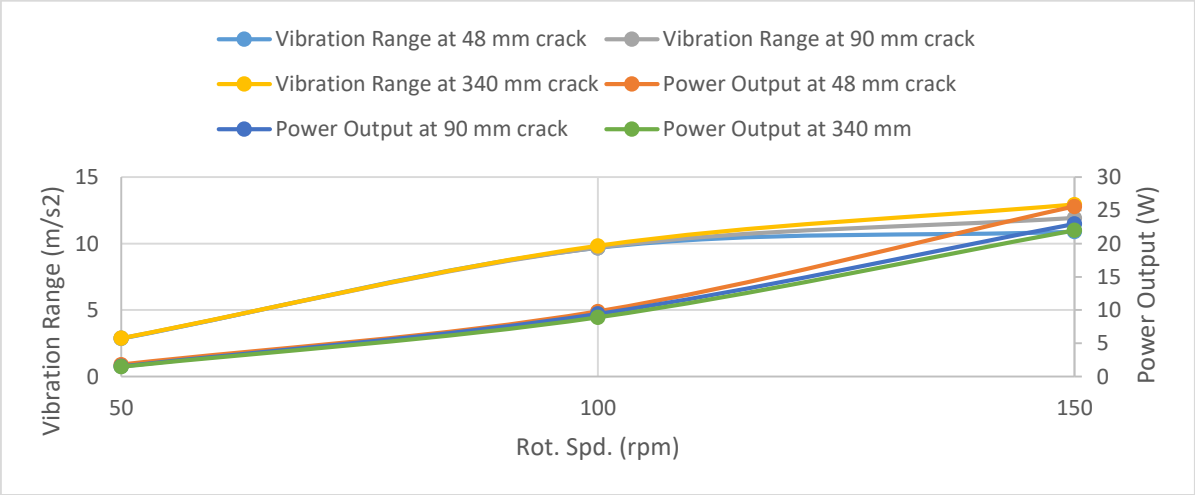

Figures 8. Vibration range and power output variation

Table 4. Response Table for the average of negative peaks

Level	Means		Signal to Noise Ratios	
	x_1	x_2	x_1	x_2
1	3.053	5.611	8.2733	14.9801
2	2.872	1.973	7.0083	5.8912
3	2.673	1.015	4.9424	-0.6473
Delta	0.380	4.596	3.3309	15.6274
Rank	2	1	2	1

3.3.3. Taguchi's Response Analysis for the average of positive peaks

In this case, the process parameters of crack size (x_1) and rotation speed (x_2) were compared to the average of the positive side of the vibration waveform peaks. Changes in either factor (x_1 or x_2) had an effect on the WTS's performance, as Table 5's Mean and Signal to Noise Ratios demonstrated. When using the lower-the-better criterion, the research revealed that the optimal set of process parameters was (x_1-1 x_2-1) also, which equated to a rotational speed of 50 rpm and a crack size of 48 mm. The response graphs for Means and Signal to Noise Ratios' average of negative peaks are shown in Figure 10.

3.3.4. Influence of process parameters on the average of positive peaks

A similar pattern was discovered when the vibration waveform's average of its positive peaks was examined. As the size of the crack developed, the methods gradually climbed from level 1 to level 3. This implied that higher positive peak amplitudes resulted from larger cracks. But rotating speed had even another more pronounced effect. From level 1 to level 3, the Signal to Noise Ratio (SNR) dropped. This showed that there was a considerable negative correlation between higher rotational speeds and positive peaks. Similar to the impacts on negative peaks, the noticeable Delta of 4.451 highlighted how rotational speed affected this parameter more than crack size.

3.3.5. Taguchi's Response Analysis for the vibration range

The current study additionally looked at how the vibration waveform range was affected by the two process parameters: (x_1) and (x_2). Table 6 illustrates how changes in either of the two factors (x_1 or x_2) impacted the system's efficiency. The study also revealed that the optimum possible set of process parameters was (x_1-1 x_2-1), (a rotational speed of 50 rpm and a crack size of 48 mm) based on the lower-the-better criterion. The average vibration range response graphs for Means and Signal to Noise Ratios are shown in Figure 11.

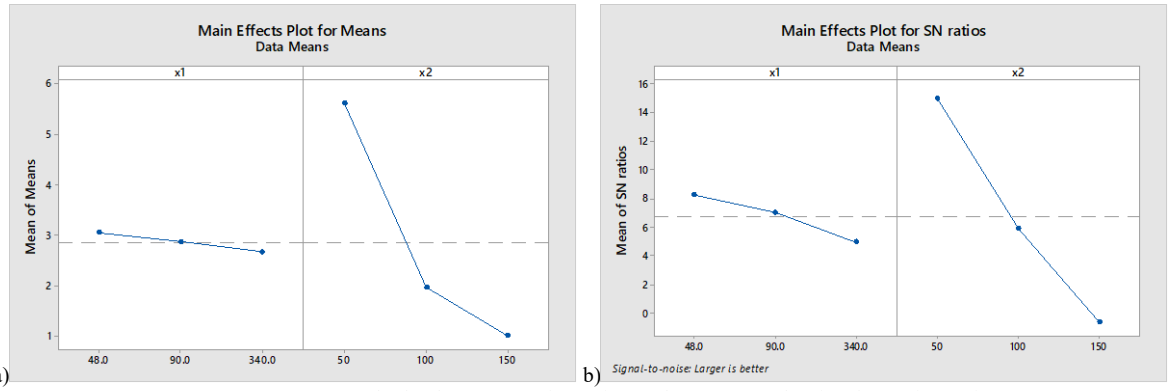

a) b)

Figure 9. Response graphs for the average of negative peaks: a) Means, b) Signal to Noise Ratios

Table 5. Response Table for the average of positive peaks

Level	Means		Signal to Noise Ratios	
	x_1	x_2	x_1	x_2
1	3.864	1.484	-10.460	-3.425
2	4.037	4.707	-10.759	-13.456
3	4.225	5.935	-11.108	-15.446
Delta	0.362	4.451	0.649	12.021
Rank	2	1	2	1

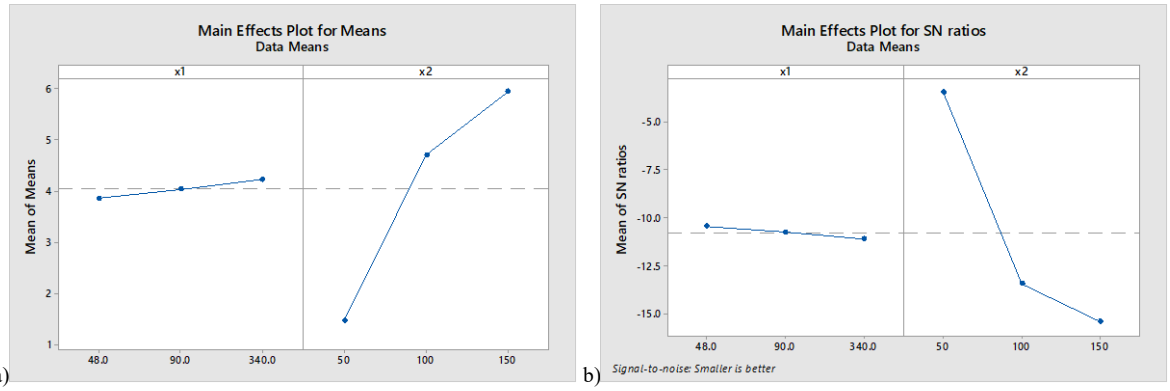

a) b)

Figure 10. Response graphs for the average of positive peaks: a) Means, b) Signal to Noise Ratios

3.3.6. Influence of process parameters on the vibration range

The vibration range analysis further reinforced the conclusion regarding the dominant role of rotational speed. As crack size increased, the average vibration range also rose. This suggested that larger cracks contributed to a wider range of vibration. The Delta value of 0.742 indicated a consistent effect but the influence of rotational speed was markedly more significant. With a Delta of 9.241, the widening of the vibration range at higher speeds (from 2.873 to 11.920) highlighted that the increased rotational speeds led to substantial enhancements in the vibration profile, which correlated with the turbine's operational dynamics.

3.3.7. Taguchi's Response Analysis for the power output

The impact of the two process parameters on the power output was also tested. Changes in each factor (x_1 and x_2) had an effect on the system's performance, as Table 7's Mean and Signal to Noise Ratio numbers demonstrate. Based on the higher-the-better criterion, the research revealed that the optimal practicable set of process parameters was (x_1-1 x_2-3). This suggested a rotational speed of 150 rpm and a crack size of 48 mm. The response graphs for the power output for Means and Signal to Noise Ratios are shown in Figure 12.

Table 6. Response Table for vibration range

Level	Means		Signal to Noise Ratios	
	x_1	x_2	x_1	x_2
1	7.811	2.873	-16.525	-9.167
2	8.165	9.735	-16.815	-19.766
3	8.552	11.920	-17.097	-21.504
Delta	0.742	9.047	0.572	12.337
Rank	2	1	2	1

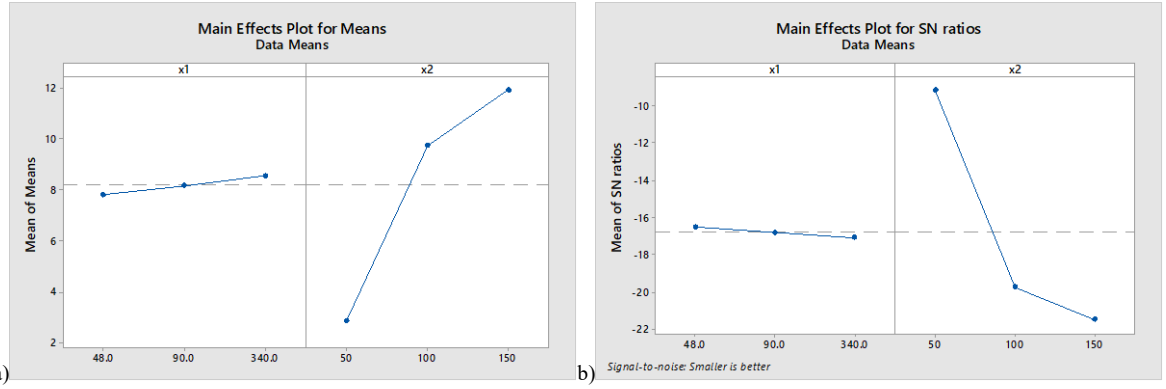

a) b)

Figure 11. Response graphs for vibration range: a) Means, b) Signal to Noise Ratios

Table 7. Response Table for power output

Level	Means		Signal to Noise Ratios	
	x_1	x_2	x_1	x_2
1	12.391	1.607	17.700	4.088
2	11.305	9.376	16.815	19.433
3	10.791	23.504	16.412	27.405
Delta	1.600	21.897	1.289	23.317
Rank	2	1	2	1

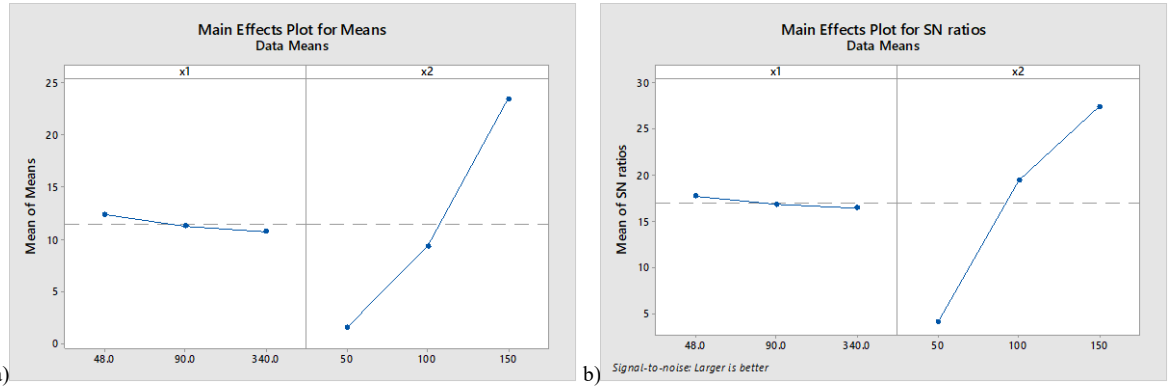

a) b)

Figure 12. Response graphs for the power output: a) Means, b) Signal to Noise Ratios

3.3.8. Influence of process parameters on the power output

The effects of these parameters were considerably more evident when looking at the generated power output. The power output continuously dropped as the crack size rose. Larger cracks have a negative effect on the capacity to produce energy, as demonstrated by a Delta of 1.600. On the other hand, rotational speed had a largely favourable effect. The mean power output increased significantly with increasing rotational speeds, rising from 1.607 at level 1 to a high of 23.504 at level 3, with a Delta value of 21.897.

3.4. Analysis of variance for measured performance

The input parameters, rotational speed (x_2) and crack size (x_1) had a significant impact on the system's reactions, as demonstrated by the analysis of variance (ANOVA) for the observed performance in WTS[44]. Minitab statistical software was used to construct an ANOVA at a 95% confidence level for the performance metrics. An ANOVA in this case showed that rotational speed (x_2) was the most important factor affecting the power output as well as the vibration range [45]. On the other hand, a statistically secondary role effect was seen for crack size (x_1). This analysis is displayed in Table 8.

With continuously high F-values and extremely low p-values across the board, the ANOVA findings showed that rotational speed (x_2) was the highest significant factor influencing all of the performance measures in the wind turbine simulator[44]. While crack size (x_1) was less important, it was more significant on the power output and largely significant on the vibration range[11]. But if the WTS runs for a longer period of time, its relevance is taken into account.

3.5. Multi-Regression modelling results

This section presents the results of a regression analysis that quantified the link between the average of negative peaks, average of positive peaks, vibration range, and power output as responses, and the crack size (x_1) and shaft rotational speed (x_2) as predictors. To find the best model fit for WTS performance, four different kinds of regression models were created. Minitab software was utilized for the regression analysis[21]. Each model's input variables are displayed in Table 9. To choose the best-fit model, the coefficient of determination (R-squared) values of the created models were compared, as Table 10 illustrates.

Table 8. Analysis of variance (ANOVA) analysis

Response	Source	DF	Adj SS	Adj MS	F-Value	P-Value
Average of negative peaks	x_1	2	0.2165	0.1082	1.39	0.348
	x_2	2	35.2714	17.6357	226.39	0.000
	Error	4	0.3116	0.0779		
	Total	8	35.7995			
Average of positive peaks	x_1	2	0.1964	0.0982	1.10	0.416
	x_2	2	31.7151	15.8575	177.48	0.000
	Error	4	0.3574	0.0893		
	Total	8	32.2689			
Vibration range	x_1	2	0.825	0.4127	1.29	0.369
	x_2	2	133.708	66.8538	209.32	0.000
	Error	4	1.278	0.3194		
	Total	8	135.811			
Power output	x_1	2	4.003	2.002	2.39	0.207
	x_2	2	739.456	369.728	441.63	0.000
	Error	4	3.349	0.837		
	Total	8	746.808			

Table 9. Regression models for vibration range and power output

Regression model	Input variables
Linear	Linear: x_1: Crack size, x_2: Rotational speed,
Linear + Squared	Linear: x_1: Crack size, x_2: Rotational speed, Squared: x_1^2: Crack size^2, x_2^2: Rotational speed^2
Linear + interaction	Linear: x_1: Crack size, x_2: Rotational speed, Interaction: Crack size × Rotational Speed ($x_1 \times x_2$)
Full quadratic (Linear + Squared + Interaction)	Linear: x_1: Crack size, x_2: Rotational speed, Squared: x_1^2: Crack size^2, x_2^2: Rotational speed^2 Interaction: Crack size × Rotational Speed ($x_1 \times x_2$)

Table 10. R^2 values of various developed regression models

Regression model	R^2 values (%)			
	Average of negative peaks (m/s^2)	Average of positive peaks (m/s^2)	Vibration range (m/s^2)	Power output (W)
Linear	89.021	92.641	90.932	96.675
Linear + Squared	99.130	98.892	99.059	99.552
Linear + interaction	89.680	93.261	91.573	96.919
Full quadratic (Linear + Squared + Interaction)	99.789	99.512	99.700	99.795

From these developed regression models shown in the Table 10, the full quadratic model showed the best fit. The regression equations for the responses are:

$$\text{Average of negative peaks} = 4.884 - 0.00289\,x_1 - 0.14826\,x_2 + 1.2\times10^{-5}x_1^2 + 0.000536\,x_2^2 - 3.1\times10^{-5}x_1\times x_2 \quad (10)$$

$$\text{Average of positive peaks} = -3.711 + 0.00290x_1 + 0.01198x_2 - 1.2\times10^{-5}x_1^2 - 0.000399x_2^2 + 2.8\times10^{-5}x_1\times x_2 \quad (11)$$

$$\text{Vibration range} = -8.60 + 0.0058x_1 + 0.2681x_2 - 2.4\times10^{-5}x_1^2 - 0.000935x_2^2 + 5.9\times10^{-5}x_1\times x_2 \quad (12)$$

$$\text{Power output} = 1.33 - 0.0286x_1 - 0.0218x_2 + 8.2\times10^{-5}x_1^2 + 0.001272x_2^2 - 8.5\times10^{-5}x_1\times x_2 \quad (13)$$

3.6. Optimization and sensitivity analysis

This study set out to balance the power output and reduce vibration levels in order to maximize the performance of the wind turbine system. Using a full factorial design in Minitab software and Grey Relational Analysis (GRA), the optimization procedure was carried out. The process of optimization led to the definition of the optimal process parameter configurations[34][45]. The GRA prioritized two main goals: reducing vibration level (lower-the-better) and increasing power output (higher-the-better). The range between the average of the positive and negative peaks in this instance is the vibration level (range). This indicated that during the optimization process, only the vibration range and power output responses are taken into account. For every experimental test, a Grey Relational Grade (GRG) was calculated using these parameters. Table 11 shows the calculated Rey Relation Coefficients GRCs and GRG values, and ranking.

Table 11. Calculated GRCs, GRG values and ranking

Experiments	Grey Relation Coefficients (GRCs)		GRG	Rank
	Vibration Range	Power Output		
1	1.000	0.336	0.668	2
2	0.425	0.433	0.429	7
3	**0.385**	**1.000**	**0.693**	**1**
4	0.995	0.334	0.664	3
5	0.425	0.427	0.426	8
6	0.357	0.821	0.589	5
7	0.994	0.333	0.664	4
8	0.419	0.420	0.420	9
9	0.333	0.771	0.552	6

The GRG created a single performance score by combining the GRCs. With a GRG of 0.693, Test 3 (x_1-1x_2-3) ranked highest. This indicated the optimal setting of a crack size of 48 mm and a rotating speed of 150 rpm. The best overall performance was represented by this set of input combinations [45]. Test 3 was the most optimum scenario since it obtained a greater GRG and provided the best balance between power output and vibration management. Table 14 displays the results confirmed. For GRG, the regression equation is:

$$\text{GRG} = 1.36 - 9.1\times10^{-4}x_1 - 0.01706x_2 + 3\times10^{-6}x_1^2 + 8.5\times10^{-5}x_2^2 - 4\times10^{-6}x_1\times x_2 \quad (14)$$

Table 14. Initial and optimal setting for WTS performance analysis

	Initial setting	Optimal setting
Parameters and levels	x_1-1 x_2-1	x_1-1 x_2-3
Average of negative peaks (m/s^2)	-1.407	-5.472
Average of positive peaks (m/s^2)	1.448	5.425
Vibration range (m/s^2)	2.855	10.896
Power output (W)	1.804	25.575
Grey Relational Grade	0.668	0.693

Sensitivity Analysis: Using the regression equations derived in this analysis, sensitivity was evaluated through systematic perturbations of the input parameters. The range of tested values was established from the experimental conditions: crack sizes of 48, 90, and 340 mm, and rotational speeds of 50, 100, and 150 rpm. For each parameter, sensitivity was defined as the percentage change in the response variables resulting from a fixed percentage change in the input parameters[44]. This allowed for a comparative assessment of which parameter had a more substantial impact on the output variables:

- *Impact of Crack Size Changes*: An increase in crack size was observed to marginally elevate both types of average peak measurements, with a more pronounced effect when rotational speeds were maintained at their highest value[11]. For instance, when the crack size increased from 48 mm to 340 mm at a rotational speed of 150 rpm, the average of positive peaks escalated significantly, affirming the evident sensitivity of this response to crack size variations. Specifically, the sensitivity ratio indicated that a 10% increase in crack size could lead to a response upsurge ranging between 2.5% to 4.6% across the different measures, with the average of positive peaks exhibiting the most pronounced sensitivity.
- *Influence of Rotational Speed*: In contrast, variations in rotational speed notably demonstrated a more dramatic impact on the operational parameters of the WTS. As rotational speed increased from 50 rpm to 150 rpm, a significant increase in power output and vibration levels was registered. Sensitivity analysis specified that a 10% increment in rotational speed would result in an approximate 20% increase in the power output, clearly highlighting its dominant influence over the power generation capabilities of the WTS. This was corroborated by the high Delta values presented in the analysis, which further confirmed that rotational speed outstripped crack size in effect on performance metrics.
- *Combined Effects*: The interaction between these parameters was also assessed. The interaction terms in

the full quadratic regression model indicated that simultaneous variations in both crack size and rotational speed lead to synergistic effects on the vibration range and power output[11]. For example, a combined increase of 10% in both parameters yielded an approximately 25% rise in power output, driven largely by the compounded impacts of increased tension and mechanical stress during higher operational speeds.

3.7. Comparison with Previous Studies

The findings of this study were validated through a comparative analysis with recent investigations [46]-[49]. Table 15 provides a summary of the comparative analysis. This current study highlights the optimization of vibration and power output in wind turbines with axial defects using experimental setups and Taguchi-based Grey Relational Analysis. In contrast, a study achieved 83.315% fault classification accuracy using chi-square feature selection with Random Forest [46], while another study reported 97% classification accuracy with Relief and KNN under multiple fault scenarios [47]. Comparatively, an additional study identified frequency shifts caused by blade erosion and achieved 98% classification accuracy, demonstrating the efficacy of signal decomposition techniques for early fault detection [48]. Similarly, a further study used an ML-based approach leveraging ReliefF feature selection and XGBoost achieved a remarkable 99.4% accuracy, outperforming other classifiers like KNN and SVM [49]. These results collectively emphasize the value of integrating experimental insights, advanced signal processing techniques like Discrete Wavelet Transform, and AI-driven methods such as machine learning classifiers to enhance the reliability, operational performance, and predictive maintenance of wind energy systems. With these approaches, it is possible to achieve early fault detection, reduce unplanned downtime, optimize power generation, and extend the service life of critical wind turbine components, ultimately contributing to the sustainability and efficiency of renewable energy infrastructure.

Table 15. Comparative Analysis with Previous Studies

Current Study	Study ref. [46]	Study ref. [47]	Study ref. [48]	Study ref. [49]
Experimental setup, Taguchi DoE, and Grey Relational Analysis.	Chi-square feature selection with RF and SVM.	ReliefF and chi-square feature ranking with ML.	DWT signal decomposition and FFT for vibration analysis.	ReliefF-based feature selection with KNN, SVM, and XGBoost.
Optimized multi-response with R-squared values above 99% for best-fit model.	RF achieved 83.315% classification accuracy.	KNN achieved 97% classification accuracy.	DWT+FFT achieved 98% classification accuracy; detected frequency shifts due to erosion.	XGBoost achieved 99.4% accuracy, outperforming KNN and SVM.
Crack size, rotational speed, vibration, power output.	Vibration features in time-domain.	Statistical vibration features and fault diagnosis.	Frequency shifts (16 Hz to 24 Hz) and erosion detection sensitivity.	Fault conditions: healthy, cracked, eroded, twisted.
Experimental insights into managing blade defects.	Highlighted ML's role in enhancing fault diagnostics.	Advanced ML models for multi-fault classification.	Demonstrated DWT's utility for early damage detection and proactive maintenance.	Showcased ML's potential for predictive maintenance with superior fault detection.

4. Conclusions

This research investigated the effects of blade axial defects on the operational performance of wind turbine systems (WTS), with more focus on vibration levels and power output[23][43]. Through the application of advanced statistical techniques, including regression analysis and Taguchi response analysis, the variations in crack size and rotational speed were clarified on how they influenced the performance metrics of the WTS[42].

The study revealed that the presence of axial defects led to significant increases in vibration levels[39][43]. This adversely affected both the stability and efficacy of the turbine's operational performance. Specifically, the recorded average negative peaks climbed from -1.407 m/s² to -6.469 m/s² (with a 340 mm crack at 150 rpm), while average positive peaks increased from 1.448 m/s² to 6.470 m/s² under similar conditions. This demonstrated the pronounced impact of blade defects. Furthermore, power output fluctuated dramatically as being reflected with these changes. When one blade was replaced with a defective blade, the power output dropped from 25.575 W to 1.478 W at lower rotational speeds, illustrating the detrimental effect of blade integrity on energy generation.

Additionally, through sensitivity analysis, the rotational speed played an essential role in determining the WTS's overall operational dynamics. The findings indicated that increases in rotational speed from 50 rpm to 150 rpm significantly influenced the power output, with an increase from 1.804 W to 25.575 W. This underscored the strategic importance of optimizing operational speed settings. Conversely, while the crack size increased, its impact on power output was significantly overshadowed by the effect of rotational speed[9]. It detected almost a four-fold increase in power output (from 1.804 W to 25.575 W) when speed was elevated at a constant crack size.

The implications of these findings extend to the broader wind energy sector. They emphasized the critical need for robust condition monitoring systems and predictive maintenance strategies. The developed regression models, with R^2 values exceeding 99%, demonstrated exceptional predictive accuracy. For instance, the final regression equation for power output demonstrated an R^2 of 99.795 and confirmed the model's effectiveness in predicting operational performance based on varying input parameters [44]. This provided a reliable framework to forecast performance degradation and plan maintenance proactively. The capability is particularly relevant for large-scale wind farms, where early detection of blade defects can minimize downtime, reduce repair costs, and ensure consistent energy output.

Moreover, this research highlights the importance of integrating real-time monitoring tools and advanced data analytics in wind turbine management. These technologies can enhance the longevity and efficiency of wind turbines by identifying and addressing emerging defects before they escalate. The study's insights also inform design improvements, advocating for blade materials and structures that are more resistant to fatigue-induced damage.

Finally, this work bridges the gap between theoretical research and practical application, as a means to improve the reliability, efficiency, and sustainability of wind energy systems. Future research should focus on exploring advanced monitoring technologies, such as AI-driven diagnostics and the development of resilient turbine designs to mitigate further the challenges posed by structural defects.

Declarations

Ethical approval - The ethical approval declaration is not applicable.

Consent for publication - The authors consent to the publication of this manuscript.

Funding - This work did not receive any specific grant from funding agencies in the public, commercial, or not-for-profit sectors.

Availability of data and materials - Materials used in this study are available upon reasonable request from the corresponding author.

Competing interests - The authors declare that they have no competing interests.

Authors' contributions–A. H. A. designed the framework of this paper and was a major contributor to writing the manuscript. K. C. V. was a major contributor in revising and improving sections 1 and 2. V. V. K. was also a major contributor to revising the manuscript and improving sections 3 and 4. All authors read and approved the final manuscript.

Acknowledgement - The authors thank the Faculty of Engineering at Sohar University for their guidance.

References

[1] Wagner, H. H. -j. Wagner, "Introduction to wind energy systems," EPJ Web of Conferences, vol. 98, p. 04002, Jan. 2015. https://doi.org/10.1051/epjconf/20159804002

[2] Wagner, H. "Introduction to wind energy systems" EPJ Web of Conferences, vol. 246, p. 00004, Jan. 2020,. https://doi.org/10.1051/epjconf/202024600004

[3]A. A. F. Ogaili, A. A. Jaber, and M. N. Hamzah, "Wind turbine blades fault diagnosis based on vibration dataset analysis," Data in Brief, vol. 49, p. 109414, Jul. 2023. https://doi.org/10.1016/j.dib.2023.109414

[4] Polinder H.,"Overview of and trends in wind turbine generator systems", 2011 IEEE Power and Energy Society General Meeting, 1-8, 2011,https://doi.org/10.1109/PES.2011.6039342

[5] Ali H. Mhmood, Bashra Kadhim Oleiwi and Amer B. Rakan, "Optimal Model Reference Lead compensator design for electric vehicle speed control using Zebra Optimization technique," Jordan Journal of Mechanical and Industrial Engineering, vol. 17, no. 04, pp. 533–540, Nov. 2023. https://doi.org/10.59038/jjmie/170408

[6] Blaabjerg, F., and Ma, "Wind energy systems," Proceedings of the IEEE, vol. 105, no. 11, pp. 2116–2131, May 2017.https://doi.org/10.1109/JPROC.2017.2695485

[7]A. Al-Hinai, K. C. Varaprasad, and V. V. Kumar, "Analytical simulation approach to evaluate the ambient humidity effects on the performance of a wind accelerator," IOP Conference Series Earth and Environmental Science, vol. 1365, no. 1, p. 012006, Jun. 2024. https://doi.org/10.1088/1755-1315/1365/1/012006

[8] Vertical-Axis wind turbine,In MDPI eBooks, 2024.https://doi.org/10.3390/books978-3-7258-0260-9

[9] Azhar Sabah Ameed, Farag Mahel Mohammed and Ahlam Luaibi Shuraiji, "Effect of laser surface treatment on the crack growth of AL 6061 alloy under impact dynamic load,"

Jordan Journal of Mechanical and Industrial Engineering, vol. 18, no. 03, pp. 521–534, Aug. 2024, https://doi.org/10.59038/jjmie/180307

[10] Lubosny Z., "Wind turbine generator systems," in Power systems, 2003, pp. 5–18. https://doi.org/10.1007/978-3-662-10944-1_2

[11] Lotfi CHELBI, Fatma HENTATI and Amna ZNAIDI, "Analysis of fatigue life and crack growth in austenitic stainless steel AISI 304L," Jordan Journal of Mechanical and Industrial Engineering, vol. 17, no. 04, pp. 501–508, Nov. 2023. https://doi.org/10.59038/jjmie/170405

[12]J. Pacheco et al., "Experimental evaluation of fatigue in wind turbine blades with wake effects," Engineering Structures, vol. 300, p. 117140, Dec. 2023. https://doi.org/10.1016/j.engstruct.2023.117140

[13]F. Zhou, J. Yang, J. Pang, and B. Wang, "Research on control methods and technology for reduction of large-scale wind turbine blade vibration," Energy Reports, vol. 9, pp. 912–923, Dec. 2022. https://doi.org/10.1016/j.egyr.2022.12.042

[14]X. Liu, C. Lu, S. Liang, A. Godbole, and Y. Chen, "Influence of the vibration of large-scale wind turbine blade on the aerodynamic load," Energy Procedia, vol. 75, pp. 873–879, Aug. 2015. https://doi.org/10.1016/j.egypro.2015.07.196

[15]W. Teng, X. Ding, S. Tang, J. Xu, B. Shi, and Y. Liu, "Vibration Analysis for fault Detection of Wind Turbine Drivetrains—A Comprehensive Investigation," Sensors, vol. 21, no. 5, p. 1686, Mar. 2021. https://doi.org/10.3390/s21051686

[16] Ihsan A. Baqer and Wafa Abd Soud, "Vibration feature extraction and artificial neural network-based approach for balancing a multi-disc rotor system," Jordan Journal of Mechanical and Industrial Engineering, vol. 17, no. 03, pp. 429–440, Aug. 2023. https://doi.org/10.59038/jjmie/170312

[17]H. J. Sutherland, "On the Fatigue Analysis of Wind Turbines," Jun. 1999.https://doi.org/10.2172/9460

[18]J. Wang, L. Zhang, X. Huang, J. Zhang, and C. Yuan, "Initiation mechanism of transverse cracks in wind turbine blade trailing edge," Energy Engineering, vol. 119, no. 1, pp. 407–418, Nov. 2021. https://doi.org/10.32604/ee.2022.016439

[19]F. Xie and A.-M. Aly, "Structural control and vibration issues in wind turbines: A review," Engineering Structures, vol. 210, p. 110087, Apr. 2020. https://doi.org/10.1016/j.engstruct.2019.110087

[20]A. Awada, R. Younes, and A. Ilinca, "Review of vibration control methods for wind turbines," Energies, vol. 14, no. 11, p. 3058, May 2021. https://doi.org/10.3390/EN14113058

[21] U. Demircioğlu, "Classifying Cutout Shapes and Predicting Cutout Location using Regression and Classification Techniques," Jordan Journal of Mechanical and Industrial Engineering, vol. 17, no. 03, pp. 367–375, Aug. 2023. https://doi.org/10.59038/jjmie/170305

[22]A. M. Abdelrhman, M. S. Leong, S. A. M. Saeed, and S. M. A. A.-O. A. Obiadi, "A review of vibration monitoring as a diagnostic tool for turbine blade faults," Applied Mechanics and Materials, vol. 229–231, pp. 1459–1463, Nov. 2012. https://doi.org/10.4028/www.scientific.net/AMM.229-231.1459

[23] Shaymaa Abdul Khader Al-Jumaili, Malik N. Hawas and Hussein Al-Gburi, "Evaluation of the impact of surface treatment on the turbine blade performance," Jordan Journal of Mechanical and Industrial Engineering, vol. 17, no. 03, pp. 421–427, Aug. 2023, https://doi.org/10.59038/jjmie/170311

[24]S. Sheng, "Wind Turbine Gearbox Condition Monitoring Round Robin Study - Vibration Analysis," Jul. 2012. http://doi.org/10.2172/1048981

[25]Z. Liu, X. Wang, and L. Zhang, "Fault diagnosis of industrial wind turbine blade bearing using acoustic emission analysis," IEEE Transactions on Instrumentation and Measurement, vol. 69, no. 9, pp. 6630–6639, Feb. 2020. http://doi.org/10.1109/TIM.2020.2969062

[26]W. Yang, Z. Lang, and W. Tian, "Condition monitoring and damage location of wind turbine blades by frequency response transmissibility analysis," IEEE Transactions on Industrial Electronics, vol. 62, no. 10, pp. 6558–6564, Apr. 2015. http://doi.org/10.1109/TIE.2015.2418738

[27]A. Joshuva and V. Sugumaran, "A data driven approach for condition monitoring of wind turbine blade using vibration signals through best-first tree algorithm and functional trees algorithm: A comparative study," ISA Transactions, vol. 67, pp. 160–172, Feb. 2017. http://doi.org/10.1016/j.isatra.2017.02.002

[28]Y. Ou, E. N. Chatzi, V. K. Dertimanis, and M. D. Spiridonakos, "Vibration-based experimental damage detection of a small-scale wind turbine blade," Structural Health Monitoring, vol. 16, no. 1, pp. 79–96, Sep. 2016. http://doi.org/10.1177/1475921716663876

[29]I. Antoniadou, N. Dervilis, E. Papatheou, A. E. Maguire, and K. Worden, "Aspects of structural health and condition monitoring of offshore wind turbines," Philosophical Transactions of the Royal Society a Mathematical Physical and Engineering Sciences, vol. 373, no. 2035, p. 20140075, Jan. 2015. http://doi.org/10.1098/rsta.2014.0075

[30]T. Barszcz, "Standard Vibration Analysis Methods," in Applied condition monitoring, 2018, pp. 33–86.https://doi.org/10.1007/978-3-030-05971-2_2

[31]F. Xiao, C. Tian, I. Wait, Z. Yang, B. Still, and G. S. Chen, "Condition monitoring and vibration analysis of wind turbine," Advances in Mechanical Engineering, vol. 12, no. 3, p. 168781402091378, Mar. 2020. https://doi.org/10.1177/1687814020913782

[32]M. H. M. Ghazali and W. Rahiman, "Vibration Analysis for Machine Monitoring and Diagnosis: A Systematic Review," Shock and Vibration, vol. 2021, pp. 1–25, Jan. 2021. https://doi.org/10.1155/2021/9469318

[33] Chinchilla M. et al.,"Laboratory set-up for wind turbine emulation", 2004 IEEE International Conference on Industrial Technology, 2004, IEEE ICIT '04., 1, 553-557 Vol. 1, 2004.https://doi.org/10.1109/ICIT.2004.1490352

[34] Luan Mulaku and Fitim Zeqiri, "Applying image processing to implement optimization approaches," Jordan Journal of Mechanical and Industrial Engineering, vol. 17, no. 04, pp. 521–531, Nov. 2023. https://doi.org/10.59038/jjmie/170407

[35]M. R. Sarkar, S. Julai, M. J. Nahar, M. Uddin, M. Rahman, and Md. R. Tanshen, "Experimental Study of Vertical Axis Wind Turbine Performance under Vibration," International Journal of Robotics and Control Systems, vol. 1, no. 2, pp. 177–185, Jun. 2021. https://doi.org/10.31763/IJRCS.V1I2.335

[36]C. Tibaldi, T. Kim, T. J. Larsen, F. Rasmussen, R. De Rocca Serra, and F. Sanz, "An investigation on wind turbine resonant vibrations," Wind Energy, vol. 19, no. 5, pp. 847–859, Jun. 2015. https://doi.org/10.1002/WE.1869

[37]R. Shinagam, G. Ajay, L. Patta, and A. S. Gandam, "Vibration and noise studies on wind turbine generator for reduction of vibrations and noise," World Journal of Engineering, vol. 17, no. 1, pp. 134–143, Jan. 2020. https://doi.org/10.1108/wje-09-2019-0275

[38]R. Pathak, A. Wadhwa, P. Khetarpal, and N. Kumar, "Comparative Assessment of regression techniques for wind power Forecasting," IETE Journal of Research, vol. 69, no. 3, pp. 1393–1402, Jan. 2021. https://doi.org/10.1080/03772063.2020.1869591

[39] H. Aarón and Y. Maldonado, "Design, study, and comparison of a new axial fan using the Fibonacci spiral and a classic axial fan," Jordan Journal of Mechanical and Industrial Engineering, vol. 18, no. 01, pp. 75–87, Feb. 2024. https://doi.org/10.59038/jjmie/180106

[40] Assem Alkarasneh, Khaled Bataineh and Yusra Aburmaileh. "A Multi Fuzzy-based Variable Step Size P&O MPPT Algorithm for PV Systems. (2024). Jordan Journal of Mechanical and Industrial Engineering, 18(04), 795–810. https://doi.org/10.59038/jjmie/180412

[41]K. Balasubramanian, S. B. Thanikanti, U. Subramaniam, S. N, and S. Sichilalu, "A novel review on optimization techniques used in wind farm modelling," Renewable Energy Focus, vol. 35, pp. 84–96, Sep. 2020. https://doi.org/10.1016/j.ref.2020.09.001

[42] Ravikumar M, Hanumanthe Gowda, Vijay Kumar S, Reddappa H N and Suresh R, "Study on Strontium and sodium Modification Elements on microstructure, mechanical, wear and fracture behavior of AL7075 alloy by Taguchi Technique," Jordan Journal of Mechanical and Industrial Engineering, vol. 18, no. 01, pp. 145–157, Feb. 2024. https://doi.org/10.59038/jjmie/180111

[43] Ishita De, Subhasish Sarkar, Shouvik Chaudhuri, Nitesh Mondal and Niraj Kumar, "Effect of Dynamic Swiveling Torque and Eccentricity on the Design of Compensator Cylinders for a Variable Displacement Axial Piston Pump–Modelling & Simulation," Jordan Journal of Mechanical and Industrial Engineering, vol. 17, no. 02, pp. 255–268, Jun. 2023. https://doi.org/10.59038/jjmie/170209

[44] Hany Mohamed Abdu, Sayed M. Tahaa, A.Wazeer, A.M.Abd El-Mageed and Moustafa M. Mahmoud, "Application of Taguchi Method and Response Surface Methodology on machining parameters of AL MMCS 6063-TIO2," Jordan Journal of Mechanical and Industrial Engineering, vol. 17, no. 04, pp. 489–499, Nov. 2023. https://doi.org/10.59038/jjmie/170404

[45] Cong Chi Tran, Van Tuan Luu, Van Tuu Nguyen, Van Tung Tran, Van Tuong Tran and Huy Dai Vu, "Multi-objective optimization of CNC milling parameters of 7075 aluminium alloy using response surface methodology," Jordan Journal of Mechanical and Industrial Engineering, vol. 17, no. 03, pp. 393–402, Aug. 2023. https://doi.org/10.59038/jjmie/170308

[46] Ahmed Ali Farhan Ogaili, Alaa Abdulhady Jaber and Mohsin Noori Hamzah, "A methodological approach for detecting multiple faults in wind turbine blades based on vibration signals and machine learning," Curved and Layered Structures, vol. 10, no. 1, Jan. 2023. https://doi.org/10.1515/cls-2022-0214

[47] Ahmed Ali Farhan Ogaili, Alaa Abdulhady Jaber and Mohsin Noori Hamzah, "Statistically optimal vibration feature selection for fault diagnosis in wind turbine blade," International Journal of Renewable Energy Research, no. V32i3, Jan. 2023. https://doi.org/10.20508/ijrer.v13i3.14096.g8782

[48] Ahmed A. Ogaili, Mohsin N. Hamzah, Alaa Abdulhady Jaber and Ehsan Ghane, "Application of discrete wavelet transform for condition monitoring and fault detection in wind turbine blades: an experimental study," Engineering and Technology Journal, vol. 0, no. 0, pp. 1–13, Nov. 2023. http://doi.org/10.30684/etj.2023.142023.1516

[49] Ahmed Ali Farhan Ogaili, Mohsin N. Hamzah, and Alaa Abdulhady Jaber, "Enhanced fault detection of wind turbine using eXtreme gradient boosting technique based on nonstationary vibration analysis," Journal of Failure Analysis and Prevention, vol. 24, no. 2, pp. 877–895, Feb. 2024. https://doi.org/10.1007/s11668-024-01894-x